Optimization-Based Design and Implementation of Multidimensional Zero-Phase IIR Filters

Dimitry Gorinevsky, *Fellow, IEEE,* and Stephen Boyd, *Fellow, IEEE*

***Abstract*—This paper considers multidimensional infinite-impulse response (IIR) filters that are iteratively implemented. The focus is on zero-phase filters with symmetric polynomials in the numerator and denominator of the multivariable transfer function. A rigorous optimization-based design of the filter is considered. Transfer function magnitude specifications, convergence speed requirements for the iterative implementation, and spatial decay of the filter impulse response (which defines the boundary condition influence in the spatial domain of the filtered signal) are all formulated as optimization constraints. When the denominator of the zero-phase IIR filter is strictly positive, these frequency domain specifications can be cast as a linear program and then efficiently solved. The method is illustrated with two two-dimensional IIR filter design examples.**

***Index Terms*—Design automation, digital filters, infinite-impulse response (IIR) filters, iterative methods, multidimensional systems, optimization.**

I. Introduction

FILTERING of multidimensional signals is required in many diverse areas. Signal processing applications include image processing, video signal filtering, computational tomography, and more. Multidimensional filter mathematics can be also used in grid methods for solving partial differential equations, distributed control, and iterative learning control. Usual (time-domain, one-dimensional) filtering is causal; there is a preferred direction in the one dimension. For most multidimensional signals, however, there is no preferred direction for the coordinates, which often represent spatial coordinates, and not time. Thus, noncausal filters are often employed in multidimensional signal processing. Multidimensional finite-impulse response (FIR) filters are well understood, since FIR filtering, causal or noncausal, is simply a convolution of the signal with the FIR kernel. Infinite-impulse response (IIR) filtering for causal (time-domain) signals is a staple of signal processing. For one-dimensional (1-D) signals, the theory of noncausal IIR filter design and implementation is less basic than the theory of FIR filter design, but still well understood; see, e.g., [20]. Multidimensional noncausal IIR filters, the subject of this paper, are less well understood.

The contribution of this paper is to present a consistent engineering approach to implementation and formal specification-driven optimal design of multidimensional noncausal IIR filters. The implementation is based on iterative (as compared to recursive) computations. We focus on zero-phase filters, which are the most commonly used noncausal filters. In our proposed filter design approach, the design problem is formulated as a linear program (LP), which incorporates both the implementation requirements and the filter design specifications. This problem can be efficiently solved; see, e.g., [2].

Manuscript received April 11, 2004; revised November 13, 2004 and March 17, 2005. This paper was recommended by Associate Editor Y. Lian.

The authors are with the Department of Electrical Engineering, Stanford University, Stanford, CA 94305 USA (e-mail: gorin@stanford.edu).

Digital Object Identifier 10.1109/TCSI.2005.856048

A. Multidimensional Filter Implementation

We first give some background and context on the various known approaches to implementation of multidimensional filters [8], [11], [14]. Reviewing these approaches will also help to recap some of the main technical ideas utilized in this work. The two longest used and most common approaches to multidimensional filtering are Fourier transform (frequency domain) implementation and FIR filters.

Fourier transform methods can be applied to multidimensional filtering in a rectangular noncausal coordinate domain. The filter implementation involves transforming the signal into the frequency domain, using a fast Fourier transform (FFT), applying the filter as a frequency-wise multiplication, and computing an inverse Fourier transform to obtain the filtered signal. One advantage of these methods is that essentially any transfer function can be implemented. The main drawback with Fourier transform methods is that they require centralized processing of the entire multidimensional signal data array at once.

Another widely used approach in multidimensional filtering relies on FIR filters, i.e., convolution with a kernel that has finite support. Multidimensional FIR filters have several advantages. They are simple, and involve only localized computations, and so are amenable to a parallel computing implementation. They are always stable, and there is no conceptual difference between causal and noncausal FIR filters. The main drawback is that a large FIR filter order is often required to satisfy performance requirements.

It is well known in 1-D signal processing that IIR filters can have dramatically lower order than FIR filters with similar performance. This holds as well for multidimensional filters. The most often used multidimensional IIR filters are causal first quad filters. A two-dimensional (2-D) causal quad filter has the form

$$y = \sum_{m=0}^{M}\sum_{n=0}^{N} b_{mn} z_1^{-m} z_2^{-n} y + \sum_{m=0}^{M}\sum_{n=0}^{N} a_{mn} z_1^{-m} z_2^{-n} x \quad (1)$$

where $x = x(j,k)$ is a 2-D input signal, $y = y(j,k)$ is an output signal, and z_1^{-1} and z_2^{-1} are unit shift (delay) operators in the two coordinates. The variables z_1 and z_2 can be also interpreted as complex indeterminants in the discrete Laplace transform (z-transform). The convolution kernels a_{mn} and b_{mn} can be interpreted as the IIR filter numerator and denominator coefficients, respectively. We usually assume that $b_{00} = 0$, so with initial conditions properly defined, the recursive update (1) can propagate in the two positive coordinate directions starting from the corner of the rectangular domain with the two smallest coordinates. Causal recursive systems of the form (1) have a well developed theory. The main drawback is that causal first quad IIR filters (1) have suboptimal performance for noncausal 2-D signals, which limits their utility.

We consider now various approaches to noncausal IIR filter implementation. In the simplest 1-D case, an IIR filter with an input $x = x(j)$ and the output $y = y(j)$ can be presented in the form

$$\sum_{m=-M}^{M} b_m z^{-m} y = \sum_{n=-N}^{N} a_n z^{-n} x \tag{2}$$

where z^{-1} is the unit shift (delay) operator. The formal transfer functions in (2) can be introduced as

$$y = \frac{A(z)}{B(z)} x, \quad B(z) = \sum_{m=-M}^{M} b_m z^{-m}$$
$$A(z) = \sum_{n=-N}^{N} a_n z^{-n}. \tag{3}$$

In the general case, there is no simple recursive update for computing y from x in accordance with (2). A stable bounded input bounded output (BIBO) map $x \to y$ can be computed from (2) provided that the denominator polynomial $B(z)$ has no zeros on the unit circle, i.e., $B(z)|_{|z|=1} \neq 0$. This is a sufficient condition for BIBO stability and necessary condition for asymptotic stability. In that case, $B(z)$ can be factorized as

$$B(z) = B_+(z) B_-(z^{-1}) z^d \tag{4}$$

where the polynomial $B_+(z)$ includes the zeros of $B(z)$ inside the unit circle with the removed coordinate origin, the factor $B_-(z^{-1})$ has the zeros of $B(z)$ outside the unit circle, and d is an appropriate integer. Now, the output y can be represented in an easily computable form as a cascade of three operators

$$y = \frac{1}{B_-(z^{-1})} \cdot \frac{1}{B_+(z)} \cdot [z^{-d} A(z)] x. \tag{5}$$

The first operator $[z^{-d}A(z)]x$ performs a noncausal FIR filtering (convolution). The second operator is a causal stable IIR filter with transfer function $1/B_+(z)$. The third operator is an anti-causal anti-stable IIR filter $1/B_-(z^{-1})$ that can be applied by running a recursive update in the negative direction starting from the final condition. Since none of the poles (zeros of the denominator $B(z)$) is on the unit circle $|z| = 1$, both IIR updates have asymptotically converging impulse responses.

Let $r < 1$ be such that all the zeros of $B_+(z)$ are inside the circle $|z| \le r$ and all the zeros of $B_-(z^{-1})$ are such that $|z^{-1}| \le r$ (outside of the circle $|z| = r^{-1}$). Then, an impulse response of the filter (2) asymptotically decays at least as fast as $r^{|j|}$, where j is the distance from the center. Suppose that the filtering is performed on a large but finite interval. The influence of the boundary conditions (initial condition and final condition) inside the interval decays as $r^{|l|}$, where l is the distance from the left or right boundary respectively. In other words, outside of the boundary layer with the characteristic width $1/\log(1/r)$, the result of the filtering on a finite interval does not depend on the boundary conditions. Consider now a noncausal 2-D IIR filter

$$B(z_1, z_2) y = A(z_1, z_2) x \tag{6}$$
$$A(z_1, z_2) = \sum_{m=-N}^{N} \sum_{n=-N}^{N} a_{mn} z_1^{-m} z_2^{-n} \tag{7}$$
$$B(z_1, z_2) = \sum_{m=-M}^{M} \sum_{n=-M}^{M} b_{mn} z_1^{-m} z_2^{-n}. \tag{8}$$

Unfortunately, the above described approach of factorizing a univariate filter denominator polynomial cannot be generalized to 2-D noncausal filters, much less to higher-dimensional filters. There are fundamental reasons why a general bivariate polynomial $B(z_1, z_2)$ cannot be decomposed into a "causal" stable and anti-causal anti-stable polynomial factors [1]. A common approach is to limit consideration to *separable* 2-D filters, where the denominator can be factorized as

$$B(z_1, z_2) = B_1(z_1) \cdot B_2(z_2). \tag{9}$$

Each of the two univariate denominator "polynomials" $B_1(z_1)$ and $B_2(z_2)$ can be factorized similar to (4). This yields the filter implementation as a sequence of a 2-D FIR numerator filter, two causal filters for each of the two coordinates, and two anti-causal filters. Filters of the form (9) are well understood but represent a limited subset of all 2-D IIR filters.

Only two approaches to realizing general noncausal 2-D filters are known to the authors. The approach of [3] is to represent (6)–(8) as a sparse system of linear equations and solve it inside a bounded domain of the signals for given boundary conditions. The solution involves manipulating matrices of a large size (a multiple of the number of points in the domain) and involves matrix transformations to reformulate the problem as a sequence of solvable sparse matrix arithmetic subproblems.

Another approach to implementing general noncausal 2-D filters, the one which this paper follows, is based on iterative computation of the filtered signal y in (6)–(8). This approach appears to be first suggested in [6], [7]. Equations (6)–(8) are iteratively solved by computing an update

$$y(n+1) = y(n) - B(z_1, z_2) y(n) + A(z_1, z_2) x \tag{10}$$

where n is the iteration number. The steady state solution of the update (10) obviously satisfies (6). In (6), the numerator $A(z_1, z_2)$ and denominator $B(z_1, z_2)$ can be scaled by the same factor without changing the filter transfer function. Provided that $B(z_1, z_2)|_{|z_1|=1, |z_2|=1} \neq 0$ (a BIBO stability condition), this scaling factor can always be chosen such that the update (10) converges. Each step of the update involves two 2-D FIR filtering operations with the kernels $A(z_1, z_2)$ and $B(z_1, z_2)$. These use localized information and can be implemented using parallel processing. The update (10) can be stopped when the solution change brought by the iteration becomes sufficiently small.

In addition to already cited work [6], [7], the iterative update filters (though not known under such name) are used in the processing of static images, where performance requirements are relaxed but conceptual clarity is important. Examples of linear or nonlinear filtering operations achieved through iterative update include such deblurring methods as Landweber Method (based on gradient descent), Van Cittered update (least mean square update), and the nonlinear Lucy-Richardson update. These methods are well described in the textbooks [11], [14].

The iterative implementation (10) of 2-D IIR filters has been known for two decades. Despite its conceptual simplicity, it is not broadly used. One possible reason is that 2-D FIR filters are simpler to understand and implement than 2-D IIR filters. A rigorous justification of the advantages of 2-D IIR filters seems to be unavailable. This paper attempts to rectify that. Another reason is that until recently iterative implementation of 2-D IIR filters was feasible only for off-line signal processing, where computational performance is not that critical, but conceptual complexity might be. The recently evolved ability to build systolic array processors implementing the filtering iterations makes on-line 2-D IIR filtering feasible. The third reason might be the absence of filter design methods comprehensively addressing all the important engineering issues. Such design approaches are proposed in this paper.

B. Multidimensional IIR Filter Design

The main engineering issues with design of iteratively implemented 2-D IIR filters are as follows.

1) The convergence of the update is not completely clear. The update (10) can be proved to converge to a steady state [6], [7]. However, its engineering use would require accurate estimates of the convergence rate. To be practical, an iterative IIR filter should require fewer computations, counting all iterations to achieve an acceptable error, compared to an FIR filter achieving the same objective.
2) There is a need for quantifying impact of the boundary conditions. In the course of the iterations (10), the boundary condition influence might theoretically propagate into the filtering domain and critically influence the solution.
3) The design methods for noncausal multidimensional IIR filters are not well developed. There are no established methods for designing such filters against formal specification requirements including the above mentioned convergence and boundary conditions requirements along with filter performance. There could also be a need to accommodate additional requirements such as robustness to round-off error in digital implementation.

This paper addresses the three above listed issues in a constructive way. The first two issues (iteration convergence and boundary conditions) have not been integrated into a filter design procedure before. Doing so is one of the contributions of this paper. Let us discuss the third issue, filter design method, in more detail.

In the usual time-domain (1-D) digital filtering, the most basic and common approach is to use fixed form IIR filters such as Butterworth, Chebyshev, or elliptic. Given a pass or stopband these filters have a small number (one to four) of parameters, such as filter order, that can be chosen as a part of the design. The main advantage is the ease of use. A greater flexibility in accommodating custom specifications is offered by optimization-based design approaches, such as McClellan-Parks FIR filter design (`remez`, see [23]) and Yule–Walker IIR filter design (`yulewalk`; see [10]) functions in the Matlab Signal Processing Toolbox. These approaches find an optimal (in some sense) filter satisfying flexible design specifications. A key to practical usefulness of these methods is that they provide a solution quickly, enabling interactive design iterations for accommodating engineering trade-offs.

In 2-D filtering (image processing) there is a greater variety of specifications than in 1-D. The most common approaches use FIR filters; 2-D IIR filter technology is not yet considered mature. The standard 2-D FIR filter design methods implemented in the Matlab Imaging Toolbox include:

- applying a 2-D window to a 2-D inverse Fourier transform of the desired frequency response;
- designing a separable 2-D filter as a direct product of 1-D FIR filters in each coordinate;
- using the McClellan transform to design approximately circularly symmetric 2-D filter, based on a 1-D design template.

There is also work on developing more general transforms for designing 2-D filters based on 1-D prototypes [21]. The approach can be also extended toward design of 2-D IIR filters, e.g., see [24] and the references therein.

A greater flexibility in accommodating custom specifications, filter structures, and better performance for a lower filter order can be achieved using optimization-based design of 2-D filters. This is the approach we describe. For a selected filter structure, optimization-based approaches find filter weights that satisfy formal engineering specifications (design constraints) and optimize one of the filter characteristics. Once again, a key to practical usefulness of these methods is fast solution and filter structure flexibility.

There is substantial research literature on optimization-based design of filters in general and 2-D filters in particular, even if the applications seem to lag behind. We will briefly survey only the most relevant work. The optimization-based design involves frequency gridding and for 2-D filters leads to large scale problems. Reliable and fast solution is possible if a convex problem is posed [2]. Very efficient convex optimization methods, such as interior-point methods, have been developed in the last decade. These methods are scalable to large problems and can be efficiently used for filter design. In particular, modern solvers and fast hardware enables solution of very large linear programming (LP) problems. Some LP-based filter design methods were first proposed more than two decades ago, but did not find very broad use earlier apparently because of the long computational times. At present time, LP solvers provide fast solution (or a certificate proving there is no solution, if the problem is infeasible). This paper formulates an LP-based multidimensional IIR filter design.

Some of the early work on using LP for design of linear-phase 1-D FIR filters can be found in [22]. Related FIR filters design approaches, leading to LP and other convex optimization problems were studied in [27]. Optimization-based design of 2-D FIR filters has been studied in many papers. One of the ideas carried through from 1-D case is that for linear-phase FIR filters frequency response is real and linear in the design parameters, i.e., the filter weights. For example, equiripple filter design leads to an LP problem; see, e.g., [15].

A range of convex optimization formulations for 2-D filter design focused on FIR filters and IIR filters with separable denominator has been proposed and explored in [18], [17]. These require custom convex solvers, unlike an off-the-shelf LP solver used in this work. Requiring that denominator is separable limits design degrees of freedom. At the same time, a vast majority of noncausal 2-D IIR filter applications require zero-phase or linear phase filters. This includes all the design examples in [17], [18]. A very important observation is that for a symmetric zero-phase or linear-phase 2-D IIR filter, the denominator has a real positive frequency response. We will see that because of this, the filter design can be formulated as an LP problem.

It appears that an LP formulation of 2-D IIR filter design problem was first proposed almost 30 years ago in [5] (also see [8]), where an LP problem was solved at each step of the iterative design process. There was relatively little work in this area since then, despite the tremendous advancements in computational performance and LP algorithms. This paper extends the LP-based design of 2-D IIR filters from optimization of basic filter performance (ripple) to a complete engineering approach that yields practically acceptable optimized designs and is easy to use. We incorporate the filter transfer function magnitude requirements as design constraints along with the update convergence speed and boundary effect requirements. We also show how the robustness, e.g., to finite wordlength implementation, can be easily incorporated into our formulation. For two realistic 2-D IIR examples in this paper the solutions are computed in a few seconds using an off-the-shelf LP solver. The approach of this paper is closely related to distributed array control design methods in [12], [25], where similar LP problems are formulated for design of multidimensional IIR filters in a control feedback loop.

The paper outline is as follows. To establish the technical background needed for understanding of the proposed approach, Section II considers issues 2 and 3: boundary effects and formal design methods for zero-phase IIR filters. These are discussed for a better understood case of 1-D noncausal IIR filtering. In Section III, the proposed methods are extended to design of an iteratively implemented 2-D zero-phase IIR filter including issue 1, update convergence. In Section IV, we discuss practical applicability and extensions of the presented approaches and specifications. The developed design methods are demonstrated in two design examples detailed in Section V.

II. One-Dimensional Noncausal IIR Filters

This section considers the problem of designing a 1-D noncausal IIR filter. The problem is used to introduce design and analysis approach ideas. Multidimensional IIR filter design is discussed in the next section.

Consider a 1-D noncausal zero phase IIR filter. Both numerator and denominator of the filter are symmetric with respect to the zero tap delay and have the form

$$y = \frac{A(z)}{B(z)} \tag{11}$$

$$A(z) = a_0 + \sum_{n=1}^{N} a_n(z^{-n} + z^n) \tag{12}$$

$$B(z) = b_0 + \sum_{m=1}^{M} b_m(z^{-m} + z^m). \tag{13}$$

In the design, the numerator order N and denominator order M are assumed to be fixed. The weights b_j and a_j are the design parameters that are chosen to achieve filter performance, specified as

$$\left| D(w) - W(w)\frac{A(e^{iw})}{B(e^{iw})} \right| \le R(w), \qquad w \in \Omega \tag{14}$$

where $D(w), W(w)$, and $R(w)$ are given frequency weighting functions and Ω is a given frequency domain. Specification requirements of the form (14) are common for many types of filters including band-pass (low-pass, high-pass, and notch filters) and deconvolution filters (deblurring in 2-D filters).

The gain of a band-pass filter is required to be close to unity in a passband and small, close to zero, in a stopband. For an equiripple design, $W(w) = 1$ and

$$D(w) = 1, \quad R(w) = r_p, \quad w \in \Omega_p \tag{15}$$

$$D(w) = 0, \quad R(w) = r_s, \quad w \in \Omega_s \tag{16}$$

where $\Omega_p \cap \Omega_s \equiv \Omega$ is the frequency domain in (14), Ω_p is the passband domain, r_p is the passband ripple bound, Ω_s is the stopband domain, and r_s is the stopband ripple bound. A possible additional specification is that the filter frequency response magnitude is bounded on transition frequencies outside of the pass and stopband.

Specifications of the form (14)–(16) can be used to describe the four common filter design problems (all frequencies are in the $[0, 2\pi]$ range).

Low-pass filter: $\Omega_p \equiv \{w \le w_p\}, \Omega_s \equiv \{w \ge w_s\}, w_s > w_p$.

High-pass filter: $\Omega_p \equiv \{w \ge w_p\}, \Omega_s \equiv \{w \le w_s\}, w_s < w_p$.

Bandpass filter: $\Omega_p \equiv \{w_{p,1} \le w \le w_{p,2}\}, \Omega_s \equiv \{w \le w_{s,1}; w \ge w_{s,2}\}, w_{s,1} < w_{p,1} < w_{p,2} < w_{s,2}$.

Notch filter: $\Omega_p \equiv \{w \le w_{p,1}; w \ge w_{p,2}\}, \Omega_s \equiv w_{s,1} \le w \le w_{s,2}\}, w_{p,1} < w_{s,1} < w_{s,2} < w_{p,2}$.

In a deconvolution/deblurring problem, the filter should invert the blur operator $H_b(e^{iw})$ in the passband and the filter gain should be bounded in the stopband (where $|H_b(e^{iw})| \ll 1$) to limit the noise amplification. The specifications (14) take the form

$$D(w) = 1, \quad W(w) = H_b(e^{iw}), R(w) = r_p, \quad w \in \Omega_p \tag{17}$$

$$D(w) = 0, \quad W(w) = 1, \quad R(w) = r_s, \quad w \in \Omega_s. \tag{18}$$

Note that for a zero-phase filter (11)–(13) the frequency responses $A(e^{iw})$ and $B(e^{iw})$ are real. In accordance with (12), (13), these frequency responses can be expanded as

$$A(e^{iw}) = c_a^T(w)p_a, \quad B(e^{iw}) = c_b^T(w)p_b \tag{19}$$

$$c_a(w) = [1 \quad 2\cos w \quad \dots \quad 2\cos Nw]^T \tag{20}$$

$$c_b(w) = [1 \quad 2\cos w \quad \dots \quad 2\cos Mw]^T \tag{21}$$

$$p_a = [a_0 \quad a_1 \quad \dots \quad a_N]^T$$

$$p_b = [b_0 \quad b_1 \quad \dots \quad b_M]^T \tag{22}$$

where p_a and p_b are the design parameter vectors. The difference between the vectors $c_a(w)$ and $c_b(w)$ is in their size, i.e., the number of terms in the expansion.

We assume that $A(z)$ and $B(z)$ are mutually prime, i.e., do not share any roots. The frequency response of the zero-phase filter $B(e^{iw})$ is real and i.e., cannot change sign (cross zero) without the filter transfer function being unbounded (design constraint violation). As discussed above, $A(z)$ and $B(z)$ are defined up to a scaling factor, which can be always chosen such that $B(e^{iw}) > 0$ for $w \in [0, 2\pi]$. The design constraints (15), (16), can be multiplied through by real positive $B(e^{iw})$. By substituting (19), this yields constraints linear in the design parameter vectors p_a and p_b at each frequency. These convex constraints can be handled in a computationally efficient way.

Consider now an additional design requirement related to the two-sided decay of the filter impulse response and boundary condition influence. The requirement is that the impulse response decays at least as fast as $r^{|n|}$, where n is the distance from the impulse and r is a design parameter, $0 < r < 1$. The response decay ensures that boundary condition influence is limited to a boundary layer with a characteristic width

$$n_b = 1/\log(1/r). \tag{23}$$

The decay of impulse response requires that the transfer function $A(z)/B(z)$ is analytical in the annulus

$$r \le |z| \le r^{-1}, \quad r < 1 \tag{24}$$

Technical background on the two-sided z-transform leading to (24) can be bound in [20]. The transfer function analyticity means that $B(z)$ should not have zeros in the annulus (24). Unfortunately this is a nonconvex constraint and it cannot be handled in a computationally efficient way. Instead, consider a convex constraint that conveniently enforces the spatial convergence and will be further shown to be a relaxation of $B(z)$ not having zeros in the annulus (24). This constraint has the form

$$|1 - B(e^{iw})| \le t < 1. \tag{25}$$

Recall that $B(z)$ is positive and can be scaled along with $A(z)$. Choosing the scaling such that t in (25) is minimized yields

$$t = \frac{1-c}{1+c}, \quad c = \frac{\inf_{w\in[0,2\pi]} B(e^{iw})}{\sup_{w\in[0,2\pi]} B(e^{iw})}. \tag{26}$$

As discussed in [20], $B(e^{iw}) > 0$ is a necessary condition for filter BIBO stability. Thus, $c > 0$ and (25) always holds for some $0 \le t < 1$. If $t = 0$, then $B(z) \equiv 1$ and we got an FIR filter with the transfer function $A(z)$. The impulse response of the FIR filter is identically zero outside of the FIR filter support. Consider a general case of $0 \le t < 1$. One can show that smaller t in (25) guarantees faster two-sided decay of the filter impulse response. The following proposition holds.

Proposition 1: Consider an IIR filter $(A(z))/(B(z))$ (11), where a $\pm M$-tap delay symmetric denominator $B(z)$ (13) satisfies (25). Then the impulse response $h(k)$ of the IIR filter decays as

$$|h(k)| \le \beta \cdot r^{|k|}, \quad r = t^{1/M} \tag{27}$$

where β is a constant; $r = t^{1/M} < 1$ is the same as in (24); and the boundary layer width estimate (23) is $n_b = M/\log(1/t)$.

Proof: It is sufficient to prove (27) for the filter $1/B(z)$, since a cascade FIR filter $A(z)$ would not change the response decay rate. We will prove the following inequality equivalent to (27):

$$|h(k)| \le \frac{t^n}{1-t}, \quad \text{for } |k| \ge n \cdot M. \tag{28}$$

Denote $C(z) = 1 - B(z)$. For any $n > 1$

$$\frac{1}{B(z)} = [1 + C(z) + \cdots + C^{n-1}(z)] + \frac{C^n(z)}{1 - C(z)}. \tag{29}$$

The first n terms in the square brackets in the r.h.s. (29) describe an FIR filter with $\pm(n-1)M$ delay taps. The impulse response of this FIR filter is zero for $|k| > (n-1)M$. Using inverse Fourier transform to evaluate the impulse response $h(k)$ for $|k| \ge nM$ yields

$$\begin{aligned} h(k) &= \frac{1}{2\pi}\int_0^{2\pi} \frac{1}{B(e^{iw})} e^{-ikw}\, dw \\ &= \frac{1}{2\pi}\int_0^{2\pi} \frac{C^n(e^{iw})}{1 - C(e^{iw})} e^{-ikw}\, dw. \end{aligned} \tag{30}$$

Recall that in accordance with (25), $|C(e^{iw})| \le t < 1$. Hence $|(C^n(e^{iw}))/(1 - C(e^{iw}))| \le (t^n)/(1-t)$ and (28) follows immediately. Q.E.D.

The linear design constraints (19)–22 and (25) can be used for posing the filter design problem as an LP problem. In the LP problem, the linear constraints are complemented by a linear performance index. By adding t to the design variables we optimize $t \rightarrow \min$, which can be considered a requirement of the fastest possible decay of the filter impulse response. The scaling degree of freedom for $A(z)$ and $B(z)$ has been already mentioned. This scaling will come out automatically from minimizing t in (25).

The design constraints (19)–(22), (25) are frequency dependent and require frequency gridding to be included in the LP problem formulation. The formulation of the LP problem on the frequency grid can be summarized as follows:

$$(1-r_p)c_b^T(w)p_b \le c_a^T(w)p_a \le (1+r_p)c_b^T(w)p_b, \quad \text{for } w \in \Omega_p \tag{31}$$

$$-r_s c_b^T(w)p_b \le c_a^T(w)p_a \le r_s c_b^T(w)p_b, \quad \text{for } w \in \Omega_s \tag{32}$$

$$1-t \le c_b^T(w)p_b \le 1+t, \quad \text{for } w \in [0, 2\pi] \tag{33}$$

$$0 \le t \le 1 \tag{34}$$

$$t \rightarrow \min. \tag{35}$$

This LP problem should be solved for the design parameter vector

$$p = \begin{bmatrix} p_a \\ p_b \\ t \end{bmatrix}. \tag{36}$$

The designed filter (11)–(13) can be implemented in the factorized form (5) as a sequence of a noncausal FIR, causal IIR, and anti-causal IIR filters.

The described approach appears to be new and is useful for designing 1-D noncausal IIR filters. However, the main meaning of this section was to prepare a background for multidimensional filter design in the next section.

III. Design of Iteratively Implemented Multi-Dimensional IIR Filters

This section presents the main contribution of this paper in design of iteratively implemented multidimensional IIR filters. For notation simplicity, 2-D filters are considered throughout the rest of this paper. A majority of the existing applications of multidimensional filtering are in 2-D image and video processing problems (e.g., see [16]). Some three-dimensional (3-D) and four-dimensional (4-D) applications exist, such as computational tomography or time-space filtering. The design and implementation approaches presented herein are directly applicable to higher-dimensional IIR filters. The only difference in the formulation is in the number of the independent coordinate arguments. The only difference in the computational design and implementation methods is in the potentially larger number of the points in a multidimensional frequency grid.

The multidimensional IIR filter design approach in this section is an extension of the LP optimization-based design in Section II. The design is performed in the frequency domain. After frequency gridding, the design requirements are formulated as convex (linear) constraints and a linear optimization criterion. One additional concern for iteratively implemented IIR filters is the iteration convergence.

Consider a 2-D IIR filter (6)–(8). In a zero-phase filter, the numerator and denominator should have symmetry properties. To avoid excessively complex notation, let us discuss the denominator symmetry; the numerator follows the same pattern. The types of symmetry usually considered for 2-D filters include (see [14]) the following.

- 2-fold symmetry: $b_{m,n} = b_{-m,-n}$.
- 4-fold symmetry: $b_{m,n} = b_{-m,-n} = b_{-m,n} = b_{m,-n}$.
- 8-fold symmetry: $b_{m,n} = b_{-m,-n} = b_{-m,n} = b_{m,-n} = b_{n,m} = b_{-n,-m} = b_{-n,m} = b_{n,-m}$.

In all of the above symmetry cases the IIR filter denominator can be expanded similar to (13)

$$B(z_1, z_2) = \sum_{m=0}^{M_b} b_m P_m^M(z_1, z_2) \tag{37}$$

where $P_m^M(z_1, z_2)$ are the elementary polynomials defining the symmetry. The expansion (37) explicitly shows $M_b + 1$ independent filter design parameters b_m for the assumed symmetry type.

For 2-fold symmetry, the symmetric expansion polynomials can be expressed in the form

$$P_0^M(z_1, z_2) = 1 \tag{38}$$

$$P_j^M(z_1, z_2) = z_2^j + z_2^{-j}, \quad (j = 1, \dots, M) \tag{39}$$

$$P_{M+k}^M(z_1, z_2) = z_1^{l_k} z_2^{m_k} + z_1^{-l_k} z_2^{-m_k}, \quad 1 \le l_k \le M, -M \le m_k \le M \tag{40}$$

where in (40) $k = 1, \dots, M(2M+1)$. The expansion size is $M_b = 1 + M + M(2M+1)$.

For 4-fold symmetry

$$P_0^M(z_1, z_2) = 1 \tag{41}$$

$$P_j^M(z_1, z_2) = z_1^j + z_1^{-j} + z_2^j + z_2^{-j}, \quad j = 1, \dots, M \tag{42}$$

$$P_{M+k}^M(z_1, z_2) = z_1^{l_k} z_2^{m_k} + z_1^{l_k} z_2^{-m_k} + z_1^{-l_k} z_2^{m_k} + z_1^{-m_k} z_2^{-l_k}, \quad 1 \le l_k \le M, 1 \le m_k \le M \tag{43}$$

where, in (43) $k = 1, \dots, M^2$. The expansion size is $M_b + 1 = 1 + M + M^2$.

For 8-fold symmetry

$$P_0^M(z_1, z_2) = 1 \tag{44}$$

$$P_j^M(z_1, z_2) = z_1^j + z_1^{-j} + z_2^j + z_2^{-j}, \quad j = 1, \dots, M \tag{45}$$

$$P_{M+j}^M(z_1, z_2) = z_1^j z_2^j + z_1^{-j} z_2^j + z_1^j z_2^{-j} + z_1^{-j} z_2^{-j}, \quad j = 1, \dots, M \tag{46}$$

$$\begin{aligned} P_{2M+k}^M(z_1, z_2) = {} & z_1^{l_k} z_2^{m_k} + z_1^{l_k} z_2^{-m_k} + z_1^{-l_k} z_2^{m_k} \\ & + z_1^{-l_k} z_2^{-m_k} + z_1^{m_k} z_2^{l_k} + z_1^{m_k} z_2^{-l_k} \\ & + z_1^{-m_k} z_2^{l_k} + z_1^{-m_k} z_2^{-l_k} \\ & (1 \le l_k \le m_k - 1, 2 \le m_k \le M) \end{aligned} \tag{47}$$

where in (47) $k = 1, \dots, M(M-1)/2$. The expansion size is $M_b + 1 = 1 + 2M + M(M-1)/2$.

Choosing a higher type of symmetry reduces the number of filter design parameters and is desirable where the symmetry of the requirements exists. To obtain frequency responses in (37)–(47), substitute $z_1 = e^{iw_1}$ and $z_2 = e^{iw_2}$. Because of the symmetry, the imaginary parts cancel and the real expansion functions $P_m^M(e^{iw_1}, e^{iw_2})$ are combinations of the frequency cosines. In all of the considered symmetry cases, the frequency responses for the numerator and denominator in (37) can be expressed in the same general form

$$A(e^{iw_1}, e^{iw_2}) = c_a^T(e^{iw_1}, e^{iw_2}) p_a \tag{48}$$

$$c_a(z_1, z_2) = \left[P_0^N(z_1, z_2) \dots P_{N_a}^N(z_1, z_2)\right]^T \tag{49}$$

$$p_a = [a_0 a_1 \dots a_{N_a}]^T \tag{50}$$

$$B(e^{iw_1}, e^{iw_2}) = c_b^T(e^{iw_1}, e^{iw_2}) p_b \tag{51}$$

$$c_b(z_1, z_2) = \left[P_0^M(z_1, z_2) \dots P_{M_b}^M(z_1, z_2)\right]^T \tag{52}$$

$$p_b = [b_0 b_1 \dots b_{M_b}]^T. \tag{53}$$

Several typical filter design specifications can be expressed as linear frequency dependent inequalities in the design parameter vectors p_a and p_b. 2-D specifications similar to (14) take the form

$$\left| W(w_1, w_2) \cdot \frac{A(e^{iw_1}, e^{iw_2})}{B(e^{iw_1}, e^{iw_2})} - D(w_1, w_2) \right| \le R(w_1, w_2). \quad (54)$$

Equiripple magnitude specifications for bandpass filters can be expressed similar to (15), (16)

$$W(w_1, w_2) = 1, \quad D(w_1, w_2) = 1, \quad R(w_1, w_2) = r_p, \quad \text{for } \{w_1, w_2\} \in \Omega_p \quad (55)$$

$$W(w_1, w_2) = 1, \quad D(w_1, w_2) = 0, \quad R(w_1, w_2) = r_s, \quad \text{for } \{w_1, w_2\} \in \Omega_s \quad (56)$$

where Ω_p is the passband domain, r_p is the passband ripple bound, Ω_s is the stopband domain, and r_s is the stopband ripple bound. In 1-D case, the stopband and the passband are combinations of frequency intervals. In 2-D filters, Ω_p and Ω_s are two-dimensional (2-D) domains that can be defined in many different ways (e.g., band, rectangular, circle, annulus, diamond, combinations of these, etc). Some specific examples are presented in the next section.

Another type of common 2-D filter design problem is a multidimensional deconvolution problem (image deblurring). Since the filter is zero-phase, it is assumed that the frequency response $H_b(e^{iw_1}, e^{w_2})$ of the blur operator is a real function. The deblurring problem can be encoded by setting $W(w_1, w_2)$, $D(w_1, w_2)$, and $R(w_1, w_2)$ in (54) similar to (17), (18)

$$D(w_1, w_2) = 1, \quad W(w_1, w_2) = H_b(e^{iw_1}, e^{w_2})$$

$$R(w_1, w_2) = r_p, \quad \text{for } \{w_1, w_2\} \in \Omega_p \quad (57)$$

$$D(w_1, w_2) = 0, \quad W(w_1, w_2) = 1, \quad R(w_1, w_2) = r_s, \quad \text{for } \{w_1, w_2\} \in \Omega_s. \quad (58)$$

Since $B(e^{iw_1}, e^{iw_2})$ is real positive, the rational inequality (54) can be multiplied through by $B(e^{iw_1}, e^{iw_2})$ to yield frequency dependent inequalities that are linear in p_a and p_b. For an iteratively implemented 2-D IIR filter, a key design requirement is convergence of the update (10). By computing a 2-D discrete Fourier transform of (10), the iterative implementation update can be presented in the form

$$\tilde{y}(n+1) = \tilde{y}(n) - B(e^{iw_1}, e^{iw_2})\tilde{y}(n) + A(e^{iw_1}, e^{iw_2})\tilde{x} \quad (59)$$

where $\tilde{x} = \tilde{x}(w_1, w_2)$ and $\tilde{y}(n) = \tilde{y}(w_1, w_2; n)$ are the 2-D Fourier transforms of the filter input and the iterated estimate of the output respectively, n is the iteration number.

Since $B(e^{iw_1}, e^{iw_2})$ and $A(e^{iw_1}, e^{iw_2})$ in (59) are real, each frequency harmonic $\tilde{y}(w_1, w_2; n)$ follows a first-order recursive difference equation. A necessary and sufficient condition for asymptotic convergence of the update for all frequencies w_1, w_2 has the form

$$\left|1 - B(e^{iw_1}, e^{iw_2})\right| \le t < 1 \quad (60)$$

where $0 \le t < 1$ is the exponential convergence factor.

Assuming that $\tilde{y}(w_1, w_2; 0) = 0$ and summing up the difference (59) yields after k steps

$$\tilde{y}(w_1, w_2; k) = H_k(e^{iw_1}, e^{iw_2})\tilde{x}(w_1, w_2) \quad (61)$$

$$H_k(z_1, z_2) = \frac{A(z_1, z_2)}{B(z_1, z_2)} \cdot (1 - D_k(z_1, z_2)) \quad (62)$$

$$D_k(z_1, z_2) = (1 - B(z_1, z_2))^k. \quad (63)$$

Given (60), the output estimate (61) converges to the filter output $y = (A)/(B)x$ as $k \to \infty$. The multiplicative residual error D_k at step k can be evaluated as

$$|D_k(e^{iw_1}, e^{iw_2})| \le t^k. \quad (64)$$

This error should be included in the transfer function ripple specifications. Since iterative implementation convergence requires $t < 1$, in accordance with (62) and (64) the stopband ripple of the transfer function (56) only improves because of the finite iteration number.

Let d_i be an allotment (in decibels) of the passband ripple error budget for the finite number of the update iterations. The number of the iterations required to achieve that error can be estimated as

$$k = \frac{d_i}{20 \log_{10} t}. \quad (65)$$

Finally, consider the requirement of the spatial decay for the impulse response of the designed IIR filter. The spatial decay limits the influence of the boundary condition. The 2-D filter analysis of the spatial decay is very similar to the 1-D analysis of Section II (Proposition 1). It turns out that the iteration convergence condition (60) has a dual role. Reducing t improves the spatial decay of the impulse response and reduces the boundary layer simultaneously with speeding up the iteration convergence.

The following extension of Proposition 1 holds for a 2-D system.

Proposition 2: Consider a 2-D filter $(A(z_1, z_2))/(B(z_1, z_2))$ (6)–(8), where a $\pm M$-tap delay symmetric denominator $B(z_1, z_2)$ (37) satisfies (60). Then, the filter impulse response $h(k_1, k_2)$ decays as

$$|h(k_1, k_2)| \le \beta \cdot r^{\max(|k_1|, |k_2|)}, \quad r = t^{1/M} \quad (66)$$

where β is a constant. The boundary layer width in each coordinate direction can be estimated as $n_b = M/\log(1/t)$.

Proof: The proof follows from the Proposition 1 proof almost exactly and is based on the fact that

$$\frac{1}{B(z_1, z_2)} \equiv \frac{1}{1 - C(z_1, z_2)} = [1 + C(z_1, z_2) + \cdots + C^{n-1}(z_1, z_2)] + \frac{C^n(z_1, z_2)}{1 - C(z_1, z_2)} \quad (67)$$

where $C(z_1, z_2) = 1 - B(z_1, z_2)$. The n-term sum in the square brackets in the r.h.s. (67) describes an FIR filter with $\pm(n-1)M$ delay taps along each coordinate. The impulse response of this FIR filter is zero if $|k_1| > (n-1) \cdot M$ or $|k_2| > (n-1) \cdot M$. For $\max(|k_1|, |k_2| > (n-1) \cdot M$, the impulse response $h(k_1, k_2)$

can be evaluated through a 2-D inverse Fourier transform of the frequency response corresponding to the last term in the r.h.s. (67). Using the inequality $|C(e^{iw_1}, e^{iw_2})| \le t < 1$ yields

$$|h(k_1, k_2)| \le \beta \cdot t^n, \quad \text{for } \max(|k_1|, |k_2|) \ge n \cdot M \tag{68}$$

where β is a constant. This immediately leads to (66). Q.E.D.

The multidimensional IIR filter can be designed by solving an LP problem. Gridding the frequencies w_1 and w_2 makes the design requirements (54), (60) into a seres of linear constraints on the filter design parameters p_a and p_b in (48)–(53). The LP filter design can be formulated by complementing these constraints with the optimization criterion

$$t \to \min \tag{69}$$

and additional constraints $0 \le t \le 1$. The LP problem should be solved for the design parameter vector $p = [p_a^T \; p_b^T \; t]^T$. The design yields a zero-phase IIR filter with fastest possible convergence of the iterative implementation and optimized bounds on boundary effects satisfying the transfer function specifications (54).

IV. Discussion

Practical suitability of the iteratively implemented multidimensional IIR filters should be compared against more established multidimensional FIR filters. Typically, an IIR filter requires much smaller number of the delay taps to achieve the same performance specifications as a matching FIR filter. For a 2-D filter, the number of floating point operations is proportional to the squared number of the delays. For a 3-D filter, the number of operations increases cubically. This makes multidimensional IIR filters potentially attractive.

This advantage is enhanced for a systolic array implementation of the filter with a separate simple processor performing computations for each pixel, e.g., see [26]. Each processing block in a systolic array would be connected to immediate neighbors and computations using data from the remote neighbors would require several data exchange cycles. For a 2-D array, on the order of M^3 data transfers are needed to broadcast each pixel to Mth remote neighbor through nearest neighbor communication. For a 3-D IIR filter, the number of data transfers increases as M^4 and savings due to smaller filter size are even more substantial.

A downside of an iteratively implemented IIR filter is that multiple iterations are required to obtain the filter output, as compared to one-shot FIR convolution computations. The number of iterations is a multiplier for the above discussed IIR filter computation count. Note that the number of iterations does not have to be very large. It can be estimated from (65). In Example 1 of Section IV, the convergence exponent $t = 0.76$ and the iteration-related ripple budget of the filter is $d_i = -22$ dB requiring $k \approx 11$ iterations. At the same time, an IIR filter is often smaller than a comparable FIR filter by a factor of three or more, yielding an order of magnitude improvement in computational requirements. Thus, iteratively implemented IIR filters can still be attractive even with several iterations required. A systolic array implementation would have an additional utility gain.

One more note on the utility of the IIR design is that a special case of $M = 0$ in (59) yields an FIR filter and the iterative update is reduced to a single step. Considering IIR filter designs with $M \ge 1$ provides additional degrees of freedom in the design space. Improvements of a baseline FIR design can be achieved through these degrees of freedom.

Let us now discuss the LP-based filter design approach considered in the previous section. The formulated basic filter design problem can be extended to accommodate additional design requirements. One important extension is designing a filter for finite-word implementation. It is well known that even a small implementation error might result in a significant filter performance deterioration. The finite-word roundoff error can be handled as uncertainty. Consider a robust design of the filter explicitly taking this uncertainty into account and guarding against the possible undesirable effects of the roundoff error. Assume that the filter numerator and denominator operators respectively have the form $A(z_1, z_2) + \Delta A(z_1, z_2)$ and $B(z_1, z_2) + \Delta B(z_1, z_2)$, where the uncertainty operators ΔA and ΔB are zero phase because the round off implementation errors preserve the symmetry. These operators are bounded as

$$|\Delta A(e^{iw_1}, e^{iw_2})| \le \delta_A, \quad |\Delta B(e^{iw_1}, e^{iw_2})| \le \delta_B \tag{70}$$

where $\delta_A = 2^{-K} N^2/2$ and $\delta_B = 2^{-K} M^2/2$, assuming K-bit precision of implementation. With the uncertainty, the design specifications (54) take the form

$$\left| W(w_1, w_2) \cdot \frac{A + \Delta A(e^{iw_1}, e^{iw_2})}{B + \Delta B(e^{iw_1}, e^{iw_2})} - D(w_1, w_2) \right| \le R(w_1, w_2). \tag{71}$$

Given (70), the design specifications (71) can be formulated as two linear inequalities

$$\begin{aligned} & W(w_1, w_2)(A + \delta_A) \\ & \quad \le (R(w_1, w_2) + D(w_1, w_2))(B - \delta_B) \qquad (72) \\ & \quad - (R(w_1, w_2) + D(w_1, w_2))(B - \delta_B) \\ & \quad \le W(w_1, w_2)(A - \delta_A). \qquad (73) \end{aligned}$$

Gridding the frequencies w_1 and w_2 in (72), (73), (60), and including (69) yields an LP problem for the filter design parameters p_a and p_b in (48)–(53).

In the proposed design approach, the ripple bound $R(w_1, w_2)$ in (54) or (72), (73), must be given in advance. If the filter order M, N and bound $R(w_1, w_2)$ are both very small, the LP problem can become infeasible. The infeasibility is reported by the standard LP solvers. Depending on the hierarchy of the design priorities, the constraints on ripple bounds and the prescribed filter order can be manipulated to yield an acceptable engineering trade-off (if one exists). This can be done in logarithmic time through simple dichotomy iterations or could be a part of interactive parameter manipulation by a filter designer.

Though the proposed approach is fundamentally focused on zero-phase IIR filters, some extensions to more general filter types are possible. For instance, a linear phase IIR filter can be designed by maintaining a zero-phase denominator (with positive real frequency response) and a linear-phase numerator. Of course, in that case the expression inside the absolute value in (54) has to be pre-multiplied by the conjugate phase to make it real. In a similar way, the design could be extended toward zero-phase denominator filters that should match an arbitrary transfer function $D(w_1, w_2)$. In that case a modification of (54) with ripple conditions written separately for the real and imaginary parts of the transfer function leads to an LP problem. This is related to the approach of [4].

V. Design Examples

In this section, the IIR filter design approach of Section III is applied to two examples of 2-D IIR low-pass filter design. The examples are borrowed from [17].

1) Example 1: Circularly-Symmetric Low-Pass Filter: The first example is designing a zero-phase 2-D IIR filter with circularly symmetric low-pass magnitude response. The design specifications are of the form (55)–(56) with the low-frequency passband Ω_p and high-frequency stopband Ω_s defined as

$$\Omega_p = \left\{ \{w_1, w_2\} \in \Omega_p : \left(\sqrt{w_1^2 + w_2^2} \leq 0.425\pi \right) \right\} \quad (74)$$

$$\Omega_s = \left\{ \{w_1, w_2\} \in \Omega_s : \left(\sqrt{w_1^2 + w_2^2} \geq 0.575\pi \right) \right\}. \quad (75)$$

As a baseline, we consider a 2-D FIR filter designed in [17] for the specifications (74)–(75). In the notation of this paper, the filter from [17] has $N = 9$ two-sided tap delays in the numerator and $M = 0$ tap delays in the denominator. The 2-D FIR convolution window is of the size $(2N + 1) \times (2N + 1) = 19 \times 19$. With such 2-D FIR filter, the passband ripple of $r_p = 0.0549$ and the stopband ripple $r_s = 0.0830$ are achieved in [17].

We designed a comparable 2-D IIR filter for iterative implementation by solving an LP problem as described in Section III. The filter of the form (6)–(8) had $M = N = 3$ two-sided tap delays in the numerator and denominator. Since the specifications (74)–(75) are circularly symmetric, an 8-fold symmetry was assumed in the filter design. In accordance with (43), this leaves $N_a = M_b = 1 + 2M + M(M-1)/2 = 10$ weights for each of the two FIR filters A and B to be chosen as the result of the design. The problem statement included the iteration convergence/spatial decay condition (60) and the optimality criterion (69).

In the design, a 32×32 grid was used for the frequency-dependent functions. The grid includes 145 passband points and 763 stopband points. This is much more than 50 passband points and 279 stopband points reported in [17, Table I]. The ripple constraints in (55)–(56) were chosen as $r_p = 0.0296$ (passband ripple of 0.5 dB), and $r_s = 0.0794$ (stopband ripple of -22 dB). This provides ripple performance superior to [17] ($r_p = 0.0549$ and $r_s = 0.0830$) as long as the iterative implementation error (63) is within the allotted budget

$$d_i = 20 \log_{10} \left(\frac{1 + 0.0549}{1 + 0.0296} - 1 \right) = -32\,\text{dB}. \quad (76)$$

The filter operators $A(z_1, z_2)$ and $B(z_1, z_2)$ obtained by solving the LP design problem are illustrated in Fig. 1. The amplitude response of the designed filter is shown in Fig. 2. The CPU time for the solution using a current Wintel PC is about 2.7 s when using the medium-scale LINPROG solver in the Matlab Optimization Toolbox. In [17], the solution time for the 19×19 FIR filter with comparable performance is given

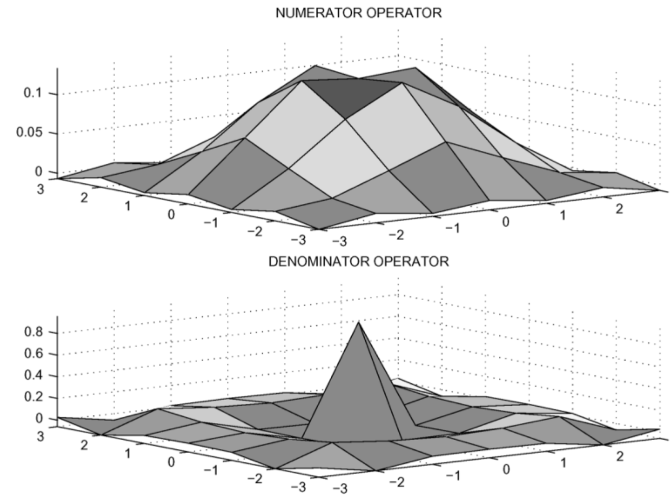

Fig. 1. Numerator A and denominator B operators for the designed circular low-pass IIR filter.

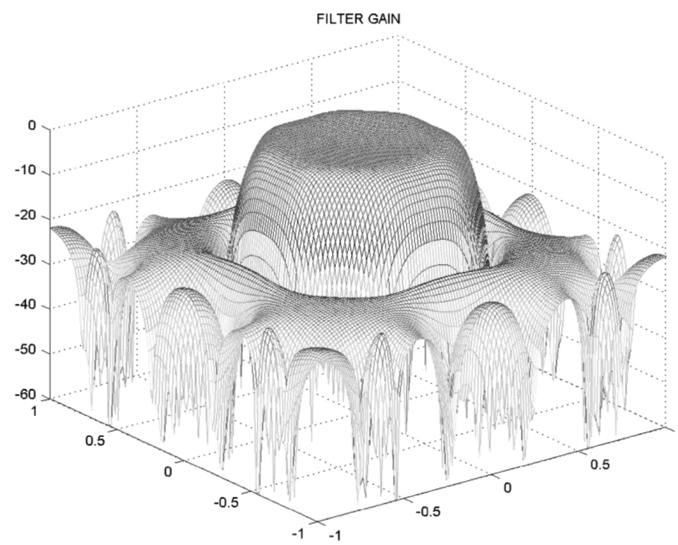

Fig. 2. Amplitude response in decibels for the designed circular low-pass IIR filter.

as 20 s. Based on the paper submission date, at least 2.5 years older and hence probably 3-4 times slower computer should be assumed in [17]. Note that the LP solver used in this work was the Matlab medium-size problem solver; for an optimized sparse solver written in "C," a 1–2 orders of magnitude computation time improvement can be expected or, alternatively, a 1–2 orders of magnitude larger problem can be solved. The main result of our implementation is that a simple Matlab code with standard solver was demonstrated to be sufficient for achieving good results.

The optimal solution yields the convergence rate t in (60) as $t = 0.7206$. With the ripple budget d_i (76) for the finite iteration error, the necessary number of iterations in (10) can be estimated as $k = (d_i)/(20 \log_{10} t) \approx 11$.

Consider now the spatial decay of the impulse response for the designed filter. The decay rate bound (66) tells that a characteristic width of response decay is no more than $-M/\log(t) \approx$ nine steps. An actual impulse response decay is shown in Fig. 3. This impulse response was computed through inverse 2-D FFT

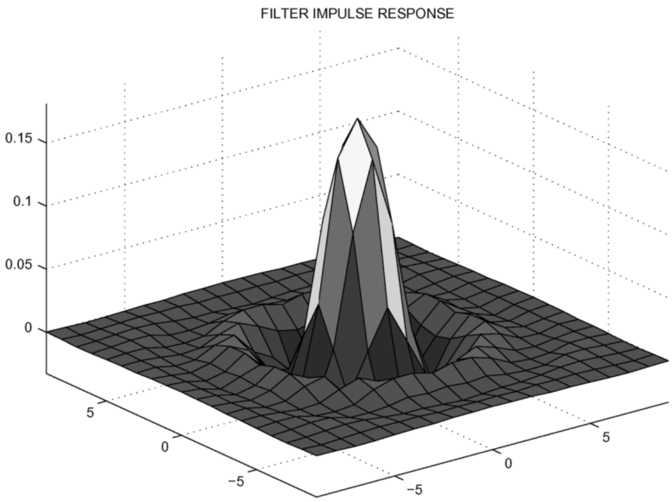

Fig. 3. Impulse response for the designed circular low-pass IIR filter.

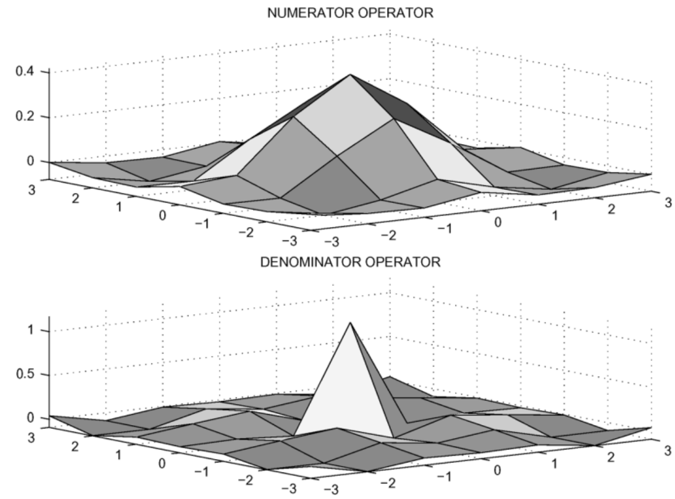

Fig. 4. Numerator A and denominator B operators for the designed diamond-shaped low-pass IIR filter.

of the frequency response $(A(e^{iw_1}, e^{iw_2}))/(B(e^{iw_1}, e^{iw_2}))$ for the designed filter. The displayed response provides a practical idea about the boundary layer effects one can expect by applying the designed 2-D IIR filter in a finite domain. The response decays off in about four steps away from the center. This is somewhat faster than the obtained bound on the asymptotic decay.

An accurate numerical estimate of whether the spatial decay specs are satisfied for given r can be done by 2-D frequency gridding and checking $H(\rho_1 e^{iv_1}, \rho_2 e^{iv_2})$, for each $\rho_j = r$ and $\rho_j = r^{-1}, j = 1, 2$. More detail and theory can be found in [13]. The condition the estimate (66) was only given to justify why minimizing t in (60) increases the decay rate of the impulse response. The actual width of the impulse response can be evaluated by computing this response explicitly. This can be quickly done as a part of the frequency-domain design by computing the impulse response as an inverse Fourier transform of the filter frequency response, such as in Fig. 3.

The designed circular 2-D filter was compared against a 2-D FIR filter designed using McClellan transformation. The prototype 1-D filter was designed as minimum-ripple 19-tap zero-phase FIR using `remez` function in the Matlab Signal Processing Toolbox and had ripple of 0.0273 in both passband and stopband. The 19×19 2-D FIR filter was designed from this prototype by using McClellan transformation (function `ftrans2` in the Matlab Image Processing Toolbox). This design yields the passband ripple $r_p = 0.0272$ and the stopband ripple $r_s = 0.1068$. The stopband ripple performance is inferior to optimization-based design in [17] ($r_p = 0.0549$ and $r_s = 0.0830$) and to our design.

Example 2: Diamond-Shaped Low-Pass Filter: The second example is designing a zero-phase 2-D IIR filter with a diamond-shaped low-passband. The design specifications have the form (55)–(56) with the passband Ω_p and stopband Ω_s defined as

$$\Omega_p = \{\{w_1, w_2\} \in \Omega_p : (|w_1| + |w_2| \le 0.8\pi)\} \quad (77)$$
$$\Omega_s = \{\{w_1, w_2\} \in \Omega_s : (|w_1| + |w_2| \ge \pi)\}. \quad (78)$$

As a baseline, we again consider a 2-D FIR filter designed in [17] for the specifications (77)–(78). The filter in [17, Table II] is a FIR convolution window of the size 19×19. When presented in the form (6)–(8) this corresponds to $N = 9$ two-sided tap delays in the numerator and $M = 0$ tap delays in the denominator. This filter in [17] achieved the ripple $r_p = 0.0496$ in the passband and $r_s = 0.0487$ in the stopband.

We designed a comparable 2-D IIR filter as described in Section III. The IIR had $M = N = 3$ two-sided tap delays in both numerator and denominator. The specifications (74)–(75) have 8-fold symmetry and the same 8-fold symmetry was assumed in the filter design. The design parameters included $1+2M+M(M-1)/2 = 10$ filter weights p_a, 10 filter weights p_b, and the iteration convergence/spatial decay parameter t in (60), (69).

The design used a 16×16 frequency grid, which included 85 passband points and 143 stopband points. This compares with 50 passband points and 121 stopband points reported in [17, Table II]. The ripple constraints in (55)–(56) were chosen as $r_p = 0.0296$ (passband ripple of 0.25 dB), and $r_s = 0.0501$ (stopband ripple of -26 dB). This is comparable to the baseline FIR design from [17]. The remaining budget of the iterative implementation error (63) was

$$d_i = 20 \log_{10} \left(\frac{1 + 0.0496}{1 + 0.0296} - 1 \right) = -34\,\text{dB}. \quad (79)$$

The designed 2-D zero-phase IIR filter operators A and B are illustrated in Fig. 4. The amplitude response of the designed filter is shown in Fig. 5. The CPU time for the design problem solution using a state of the art Wintel PC is 0.7 s with LINPROG solver from Matlab Optimization Toolbox. In [17], the solution time of 7.13 s is quoted for design of a 19×19 FIR filter with comparable performance for a computer which was likely 3–4 times slower.

The optimal solution yields the convergence rate t in (60) as $t = 0.8688$. To satisfy the ripple error budget d_i (79), $k = (d_i)/(20 \log_{10} t) \approx 34$ iterations are required.

The impulse response for the designed filter is shown in Fig. 6. This impulse response was computed through inverse 2-D FFT of the 2-D IIR filter frequency response. The response decays off in about four steps away from the center. The

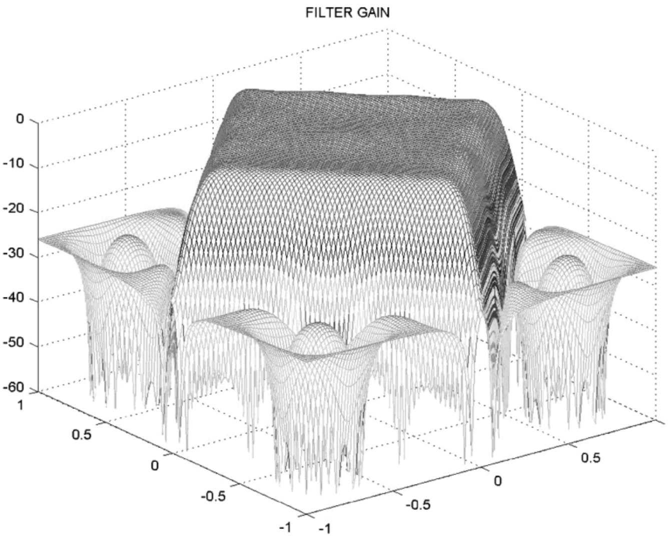

Fig. 5. Amplitude response in decibels for the designed diamond-shaped low-pass IIR filter.

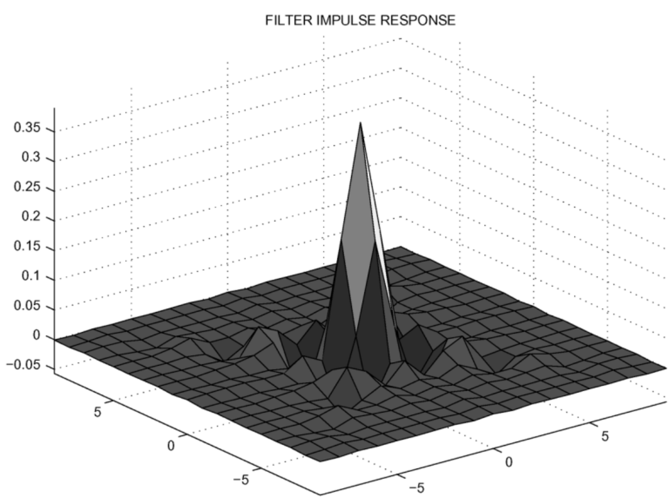

Fig. 6. Impulse response for the designed diamond-shaped low-pass IIR filter.

decay rate estimate (66) gives a larger characteristic length of response decay of about $-M/\log(t) \approx 21$ steps, but then the asymptotic decay rate in Fig. 6 appears to be slower than the initial decay in the middle of the response.

VI. Conclusion

We have proposed a new approach to noncausal multidimensional IIR filters. The approach combines optimization-based design with iterative implementation of the filters. It is an efficient alternative to existing designs of zero-phase multidimensional IIR filters. The optimization-based design formally includes various filter transfer function magnitude specifications as optimization constraints in LP problem. We have demonstrated fast filter design using off-the-shelf LP solver. Iteratively implemented multidimensional IIR filters do not need to be causal (first quad) or have a separable denominator as in other related work. We have also considered and explicitly included into the design requirements the impulse response decay that characterizes the width of the boundary effect layer in the filtered signal domain. We have demonstrated two design examples for low-pass 2-D filters with design specifications borrowed from earlier work. Even taking into account the computational expense of the iterations, the designed filters perform better or the same as the filters based on existing approaches.

References

[1] N. K. Bose, *Applied Multidimensional Systems Theory*. New York: Van Nostrand, 1982.

[2] S. Boyd and V. Vandenberghe, *Convex Optimization*. Cambridge, U.K.: Cambridge Univ. Press, 2004.

[3] M. M. Daniel and A. S. Willsky, "Efficient implementations of 2-D noncausal IIR filters," *IEEE Trans. Circuits Syst. II, Analog Digit. Signal Process.*, vol. 44, no. 7, pp. 549–563, Jul. 1997.

[4] A. Chottera and G. Jullien, "Design of two-dimensional recursive digital filters using linear programming," *IEEE Trans. Circuits Syst.*, vol. CAS-29, no. 12, pp. 817–826, Dec. 1982.

[5] D. E. Dudgeon, "Two-dimensional recursive filter design using differential correction," *IEEE Trans. Acoust., Speech, Signal Process.*, vol. ASSP-23, no. 3, pp. 264–267, Mar. 1975.

[6] ——, "An iterative implementation of 2-D digital filters," *IEEE Trans. Acoust., Speech, Signal Process.*, vol. ASSP-28, no. 6, pp. 666–671, Jun. 1980.

[7] D. E. Dudgeon and T. F. Quatieri, "Implementation of 2-D digital fibers by iterative method," *IEEE Trans. Acoust., Speech, Signal Process.*, vol. ASSP-30, no. 3, pp. 473–487, Mar. 1981.

[8] D. E. Dudgeon and R. M. Mersereau, *Multidimensional Digital Signal Processing*. Englewood Cliffs, NJ: Prentice-Hall, 1984.

[9] M. Ekstrom, R. Twogood, and J. Woods, "Two-dimensional recursive filter design—A spectral factorization approach," *IEEE Trans. Acoust., Speech, Signal Process.*, vol. ASSP-28, no. 1, pp. 16–26, Jan. 1980.

[10] B. Friedlander and B. Porat, "The modified Yule-Walker method of ARMA spectral estimation," *IEEE Trans. Aerosp. Electron. Syst.*, vol. AES-20, no. 2, pp. 158–173, Feb. 1984.

[11] R. C. Gonzales and R. E. Woods, *Digital Image Processing*, 2nd ed. New York: Addison-Wesley, 1993.

[12] D. Gorinevsky, S. Boyd, and G. Stein, "Optimization-based tuning of low-bandwidth control in spatially distributed systems," in *Proc. Amer. Control Conf.*, vol. 3, Denver, CO, Jun. 2003, pp. 2658–2663.

[13] D. Gorinevsky and G. Stein, "Structured uncertainty analysis of robust stability for multidimensional array systems," *IEEE Trans. Autom. Control*, vol. 48, no. 8, pp. 1557–1568, Aug. 2003.

[14] J. S. Lim, *Two-Dimensional Signal and Image Processing*. Englewood Cliffs, NJ: Prentice-Hall, 1990.

[15] J. H. Lodge and M. F. Fahmy, "An efficient l_p optimization technique for the design of two-dimensional linear phase FIR digital filters," in *IEEE Trans. Acoust., Speech, Signal Process.*, vol. ASSP-28, Mar. 1980, pp. 308–313.

[16] J. Konrad, J. Radecki, and E. Dubois, "The application of two-dimensional finite-precision IIR filters to enhanced NTSC coding," *IEEE Trans. Circuits Syst. Video Technol.*, vol. 6, no. 4, pp. 355–374, Apr. 1996.

[17] W.-S. Ln, "A unified approach for the design of 2-D digital filters via semidefinite programming," *IEEE Trans. Circuits Syst. I, Fundam. Theory Appl.*, vol. 49, no. 6, pp. 814–826, Jun. 2002.

[18] W.-S. Lu, S.-C. Pei, and C.-C. Tseng, "A weighted least-squares method for the design of stable 1-D and 2-D IIR digital filters," *IEEE Trans. Signal Process.*, vol. 46, no. 1, pp. 1–10, Jan. 1998.

[19] M. D. Lutovac, D. V. Tosic, and B. L. Evans, "Advanced digital IIR filter design," in *Proc. 31st Asilomar Conf. Signals, Syst., Comput.*, vol. 1, Nov. 2–5, 1997, pp. 710–715.

[20] A. V. Oppenheim, R. W. Schafer, and J. R. Buck, *Discrete-Time Signal Processing*. Englewood Cliffs, NJ: Prentice-Hall, 1999.

[21] S.-C. Pei and J.-J. Shyu, "Design of 2D FIR digital filters by McClellan transformation and least squares eigencontour mapping," *IEEE Trans. Circuits Syst. II, Analog Digit. Signal Process.*, vol. 40, no. 9, pp. 546–555, Sep. 1993.

[22] L. Rabiner, N. Graham, and H. Helms, "Linear programming design of IIR digital filters with arbitrary magnitude function," *IEEE Trans. Acoust., Speech, Signal Process.*, vol. ASSP-22, no. 2, pp. 117–123, Feb. 1974.

[23] L. R. Rabiner, J. H. McClellan, and T. W. Parks, "FIR digital filter design techniques using weighted Chebyshev approximations," *Proc. IEEE*, vol. 63, no. 4, pp. 595–610, Apr. 1975.

[24] B. A. Shenoi and P. Misra, "Design of two-dimensional IIR digital filters with linear phase," *IEEE Trans. Circuits Syst. II, Analog Digit. Signal Process.*, vol. 42, no. 2, pp. 124–129, Feb. 1995.

[25] G. Stein and D. Gorinevsky, "Design of surface shape control for large two-dimensional array," *IEEE Trans. Control Syst. Technol.*, vol. 13, no. 3, pp. 422–433, Mar. 2005.

[26] L.-D. Val, "A new 2-D systolic digital filter architecture without global broadcast," *IEEE Trans. Very Large Scale Integr. (VLSI) Syst.*, vol. 10, no. 4, pp. 477–486, Apr. 2002.

[27] S.-R. Wu, S. Boyd, and L. Vandenberghe, "FIR filter design via spectral factorization and convex optimization," in *Applied and Computational Control, Signals and Circuits*. Berlin, Germany: Birkhauser, 1997, ch. 2, pp. 51–81.

Dimitry Gorinevsky (M'91–SM'98–F'06) received the M.Sc. degree from the Moscow Institute of Physics and Technology, Moscow, Russia, in 1982, and the Ph.D. degree from the Department of Mechanics and Mathematics, Moscow (Lomonosov) University, Moscow, Russia, in 1986.

He is a Consulting Professor of Electrical Engineering at Stanford University, Stanford, CA. He was with Honeywell from 1995 until 2005. Prior to that, he held research, engineering, and academic positions in Moscow, Russia; Munich, Germany; and Toronto and Vancouver, Canada. His interests are in signal processing, decision, and control systems applications across many industries. He has authored a book, more than 130 reviewed technical papers, and a dozen patents.

Dr. Gorinevsky is an Associate Editor of the IEEE TRANSACTIONS ON CONTROL SYSTEMS TECHNOLOGY. He was a recipient of the Control Systems Technology Award in 2002, and the IEEE TRANSACTIONS ON CONTROL SYSTEMS TECHNOLOGY Outstanding Paper Award of the IEEE Control Systems Society in 2004.

Stephen Boyd (F'98) received the B.A. degree in mathematics from Harvard University, Cambridge, MA, in 1980, and the Ph.D. degree in electrical engineering and computer science from the University of California, Berkeley, in 1985.

He then joined the faculty at Stanford University, Stanford, CA, where he is currently the Samsung Professor of Engineering, and Professor of Electrical Engineering in the Information Systems Laboratory. His current research focus is on convex optimization applications in control, signal processing, and circuit design.